A Bidirectional Fixed-Bed Reactor for Coupling of Exothermic and Endothermic Reactions

Milind S. Kulkarni and Milorad P. Duduković
Chemical Reaction Engineering Laboratory, Dept of Chemical Engineering,
Washington University, St. Louis, MO 63130

Performance of a bidirectional fixed-bed reactor subject to both flow reversal and switching between exothermic and endothermic reactions is simulated. During odd semicycles (blows) an exothermic reaction heats the bed, during even semicycles an endothermic reaction cools the bed and produces the desired product in the hot zone. Such an operation is possible and efficient when the inlet gas temperature is lower than the initial bed temperature, leading to the wrong-way behavior when the temperature front moves with a finite velocity (creep velocity) from the feed end to the exit during a semicycle. Since the dynamic nature of the fixed-bed reactor changes with each semicycle, the front velocity during an exothermic semicycle differs from the front velocity during an endothermic semicycle and an asymptotic expression is developed for the differential creep (front) velocity that quantifies this difference. Due to a nonzero differential creep velocity, the front exhibits an effective displacement after each cycle. This asymptotic expression for the creep velocity works very well except in the inlet and outlet region of the fixed-bed reactor. An expression developed for 100% energy efficiency shows that it can be reached only if the differential creep velocity is zero. A relation for the balanced operation of a reactor-regenerator is discussed as well as differences in reactor performance caused by reactions occurring in the gas or solid phase.

Introduction

Modeling the dynamic operation of fixed beds

The processes dealing with heat storage in, and recovery from, packed beds received early attention. Among others Anzelius, Nusselt, Schumann, Hausen, Schmeidler and Ackermann (Jakob, 1957), and Schmidt and Willmott (1981) studied the dynamic operation of packed-bed heat regenerators without reactions. Ermenc (1956a,b) added the possibility of running reactions in such systems and developed *The Wisconsin Process* for the thermal production of nitric oxide in which the cold reactants (nitrogen and oxygen in air) were heated and the products (NO + unreacted air) were cooled using heat regenerators. Levenspiel (1988) used the dispersion model to explain the spreading of the temperature front in a heat regenerator without reaction, while Ramachandran and Duduković (1984) developed a moving finite-element collocation method for moving fronts in heat regenerators. They also solved the linear regenerator model using triple collocation, that is, collocation in space and time, and developed the design criteria for periodic operation of heat regenerators (Duduković and Ramachandran, 1984).

Rhee et al. (1973), Matros (1989), Eigenberger and Butt (1988), and Gupta and Bhatia (1991) are among many who studied the dynamic operation of fixed-bed reactors. Rhee et al. (1973) developed an approximate expression for the temperature front. Matros (1989) showed that the yield of a thermodynamically reversible mildly exothermic catalytic reaction can be increased subject to forced flow reversal. Matros (1989), Snyder and Subramaniam (1993), Bunimovich et al. (1995), and others studied SO_2 oxidation in the solid phase in a reverse-flow reactor. Eigenberger and Nieken (1988) investigated the catalytic combustion of hydrocarbons with periodic flow reversal using the Crank–Nicolson numerical algorithm developed by Eigenberger and Butt (1976). Agar and Ruppel (1988) used an implicit finite-difference approximation to study NO_x removal in the presence of ammonia and air by forced flow reversal in a fixed-bed reactor. Gawdzik and Rakowski (1988, 1989), using a combination of the method of characteristics and orthogonal collocation, investigated the operation of an adiabatic tubular reactor forced through the reversal of flow of the reaction mixture. Blanks et al. (1990) employed numerical simulation as well as a series of experiments in studying the production of synthesis gas by flow reversal. Gupta and Bhatia (1991) simulated the reactor cyclic operation by using collocation on finite elements in space and treated the differential equation system as a boundary-value problem in time, with the stationary catalyst temperature profiles at the beginning and at the end of a half-cycle being mirror images of each other. Wallace and Viljoen (1995) modeled the oxidation of CO in a monolithic catalytic bed with reciprocating flow.

All of the literature just cited deals with the cyclic operation of fixed-bed regenerators and fixed-bed reactors. A typical cyclic operation of a fixed-bed reactor involves two semicycles. During a semicycle, the reactants are fed into the fixed-bed reactor from one end and during the next semicycle the reactants are fed into the bed from the other end. These repeated swings, or flow-reversals, of the feed result in an inverted U-shaped temperature profile that travels in the bed from one position to another. The references cited so far discussed only the bidirectional fixed-bed reactors subject to the same type of reaction throughout the cyclic operation, that is, the same feed is introduced into the reactor during two successive semicycles. For example, in the catalytic oxidation of SO_2 the type of reaction that occurs in the fixed-bed reactor is always catalytic oxidation of SO_2 during every semicycle. The type of reaction does not change with the flow reversal of the feed (Matros, 1989; Eigenberger and Nieken, 1988). Thus, the thermodynamic and dynamic nature of the system does not change with flow reversal.

The RE-GAS process

Levenspiel (1988) proposed the *RE-GAS* process to produce synthesis gas. The process can involve gas-phase or solid-phase reactions. The fixed-bed reactor now also acts like a heat regenerator. The *odd blow*, or the *odd semicycle*, involves feeding gaseous reactants that react exothermally in the fixed-bed reactor. During the *even blow*, or the *even semicycle*, another gaseous mixture, which contains reactants that undergo an endothermic reaction, is introduced from the opposite end of the bed. The product of interest is the product of the endothermic reaction that is carried out in the hot bed. The general idea is that the even blow is allowed to go on until the bed is sufficiently cooled down. These two semicycles constitute one complete cycle that is periodically repeated. For example, in the production of synthesis gas by the RE-GAS process, even blows involve heating the bed by burning a hydrocarbon fuel, and odd blows involve the production of synthesis gas by endothermic reactions between steam and CO_2. The synthesis gas produced by this process is not diluted with N_2 unlike in the bidirectional process proposed by Blanks et al. (1990).

In the RE-GAS process, the type of reaction that takes place in the bed changes with each semicycle. Thus, two successive semicycles do not lead to mirror-image solutions during the pseudo steady state. The parameters like the maximum temperature and front velocity are different for even and odd semicycles. So far asymmetric bidirectional fixed-bed reactors subject to different reactions during even and odd semicycles have not been studied. Hence, there is a need to study RE-GAS type of processes in order to develop an understanding of asymmetric fixed-bed operation under these new flow-reversal conditions. This is the objective of the present study.

Quantities of Interest

There are a few fundamental questions that need to be addressed for the proper understanding of the previously discussed new reverse-flow fixed-bed process. It is expected that the inlet-gas temperatures for the exothermic and endothermic reactions in relation to the initial bed temperature affect the performance of the process. Also, periods of even and odd semicycles, t^*_{even} and t^*_{odd}, respectively, should affect the yield of the process. In traditional bidirectional processes t^*_{even} is equal to t^*_{odd} because the front speeds of odd and even semicycles are equal to each other. However, in the RE-GAS-type process, due to different reactions occurring during odd and even semicycles, the velocity of the temperature front is different for the odd and even semicycles. Hence, the ratio $t^*_{\text{odd}}/t^*_{\text{even}}$ can have a significant effect on the performance of the process. The possibility of achieving 100% energy efficiency by coupling endothermic and exothermic reactions is addressed. It is also necessary to investigate the effect of the phase in which reaction occurs, that is, the process can occur mainly catalytically in the solid phase or homogeneously in the gas phase.

In this work we address the preceding questions by performing simulation studies to examine the effect of the inlet temperature ($T_{g,in}$), the phase in which the reaction occurs, and the duration of the switching time t^* on a RE-GAS type of process. The purpose of this numerical simulation is not to optimize the process but to gain physical insight into the parametric sensitivity of the RE-GAS type of process.

Gas-Phase RE-GAS-Type Process

Model

We consider a packed-bed reactor with highly exothermic and endothermic reactions occurring in the gas phase. The parametric values used in the computation (Table 1) correspond to a typical combustion and endothermic gasification system. The two reactions are:

$$\text{Exothermic:} \quad A \rightarrow C \quad \Delta H_{g,A} < 0 \ \ldots \ \text{(gas phase)}$$

$$\text{Endothermic:} \quad B \rightarrow D \quad \Delta H_{g,B} > 0 \ \ldots \ \text{(gas phase).}$$

It is assumed that only the reaction $A \rightarrow C$ occurs in the bed during an odd semicycle when reactant A is fed to the system, and only the reaction $B \rightarrow D$ takes place during an even semicycle when reactant B is fed from the opposite end of the reactor. The heats of exothermic and endothermic reactions are set to be different (Table 1) to allow for different front speeds during odd and even semicycles but are assumed constant.

A model is now developed subject to the following additional assumptions.

Table 1. Parameters Used in the Simulation of Various Processes

Parameter	Value
$T_{g,in}$ (K)	700
$T_{g,0}$ (K)	1,000
$T_{s,0}$ (K)	1,000
y_{in}	0.1
y,	Variable
k_0 (s^{-1})	1.0×10^5
Ea (J/mol)	1.0×10^5
ΔH_A (J/mol)	-2.0×10^5
ΔH_B (J/mol)	1.5×10^5
h (J/m^2·K·s)	100
C_p (J/kg·K)	1,000
ρ_s (kg/m^3)	3,000
a_p (m^2/m^3)	300
u_{in} (m/s)	1
P (Pa)	1.013×10^5
L (m)	5
ϵ	0.5
M_w	28

1. Axial dispersion of heat and mass in the gas as well as in the solid phase is assumed to be negligible. The assumption of plug flow of gas holds true for long reactors at high gas velocities. The assumption of negligible dispersion in the solid phase holds true for solid packings, which allow minimal area of contact between two solid particles. Clearly there will be some dispersion of heat in high-temperature beds by various means, including radiation, but this is neglected at present, as the zero-dispersion model represents a useful limiting case to study in illustrating the features of the process.

2. The rate of conduction within the solids is assumed to be very high compared to the convective heat-transfer rate between the gas and solids, which is a fair assumption if particles are not too large.

3. The gas is assumed to be compressible with the total mass flux of gas being constant ($\rho_g u = \rho_{g,in} u_{in}$) (Kulkarni, 1992).

4. Pore diffusion in the solids, and external mass-transfer resistances between the gas and the solids, are incorporated into the overall kinetic expression for the reaction occurring in the solid phase. Kinetics is assumed to have an Arrhenius-type dependence on the temperature and to be first order.

Admittedly the preceding model, which uses first-order Arrhenius-type kinetics that does not change over a wide range of temperature, is a great simplification of reality. Over the extended temperature range the real gas-phase reaction mechanism can change several times. Pore diffusion changes within 50 K and radiation heat-transfer effects can be very important. However, this work concerns itself with a preliminary and fundamental study of an asymmetric operation of a fixed-bed reactor. The purpose of this work is to gain a physical insight into a RE-GAS-type asymmetric process. Once the global features of the asymmetric fixed-bed reactor are well understood, the real RE-GAS process with real kinetics can be studied. The preceding numerical model is sufficient for our current purpose of understanding whether a periodic operation of asymmetric fixed-bed reactors is possible and how it is affected by initial gas temperature and characteristic reaction parameters. The model based on all the assumptions just listed should be adequate to establish the effect of $T_{g,in}$, the phase in which reaction occurs, the volumetric heat-transfer rate, and the front velocity on the RE-GAS process, all of which represent the focus of this study.

The model equations consist of the energy balance for the gas and solid phase, Eqs. 1 and 2, respectively; reactant A, B mass balances, Eqs. 3 and 4, respectively; and the overall continuity, Eq. 5:

$$\frac{\partial \theta_g}{\partial \tau} = -U\frac{\partial \theta_g}{\partial z} + \tau_{s/r,g,A} TR_{g,A}\, \gamma_{g,A}^{((1-\theta)/(\theta_g+\theta_{g,d}))} y_A$$

$$+ \tau_{s/r,g,B} TR_{g,B}\, \gamma_{g,B}^{((1-\theta_g)/(\theta_g+\theta_{g,d}))} y_B - St_g \frac{1}{\Omega_g}(\theta_g - \theta_s) \quad (1)$$

$$\frac{\partial \theta_s}{\partial \tau} = St_s(\theta_g - \theta_s) \quad (2)$$

$$\frac{\partial y_A}{\partial \tau} = -U\frac{\partial y_A}{\partial z} - \tau_{s/r,g,A}\, \gamma_{g,A}^{((1-\theta_g)/(\theta_g+\theta_{g,d}))} y_A \quad (3)$$

$$\frac{\partial y_B}{\partial \tau} = -U\frac{\partial y_B}{\partial z} - \tau_{s/r,g,B}\, \gamma_{g,B}^{((1-\theta_g)/(\theta_g+\theta_{g,d}))} y_B \quad (4)$$

$$\frac{\partial \Omega_g}{\partial \tau} = -\frac{\partial(\Omega_g U)}{\partial z} = 0. \quad (5)$$

The boundary conditions are:

$@\ z = 0$

$$\theta_g = \theta_{g,in}; \qquad y_A = Y_{A,in}; \qquad y_B = y_{B,in}.$$

The initial conditions are:

$@\ t = 0 \quad \text{and} \quad 0 \le z \le 1$

$$\theta_g = \theta_{g,0}; \qquad y_A = y_{A,0}; \qquad y_B = y_{B,0}.$$

The dimensionless quantities used above are:

$$\tau = \frac{t}{L/u_{in}}; \qquad z = \frac{x}{L}; \qquad \theta_g = \frac{T_g - T_{g,in}}{\Delta T_{ad}};$$

$$\theta_s = \frac{T_s - T_{g,in}}{\Delta T_{ad}}; \qquad \theta_{g,d} = \frac{2T_{g,in} - T_{g,in}}{\Delta T_{ad}}; \qquad \Omega_g = \frac{\rho_g}{\rho_{g,in}};$$

$$U = \frac{u}{\epsilon u_{in}}; \qquad \gamma_{g,A} = e^{(-Ea_{g,A}/RT_{g,ad})}; \qquad \gamma_{g,B} = e^{(-Ea_{g,B}/RT_{g,ad})}$$

$$\tau_{s/r,g,A} = \frac{\tau_s}{\tau_{r,g,A}} = \frac{L/u_{in}}{\left[\dfrac{1}{(k_{0,g,A}/\epsilon)e^{(-Ea_{g,A}/RT_{g,ad})}}\right]};$$

$$\tau_{s/r,g,B} = \frac{\tau_s}{\tau_{r,g,B}} = \frac{L/u_{in}}{\left[\dfrac{1}{(k_{0,g,B}/\epsilon)e^{(-Ea_{g,B}/RT_{g,ad})}}\right]}$$

$$TR_{g,A} = \frac{1{,}000(-\Delta H_{g,A})}{M_w C_{p,g} \Delta T_{ad}}; \qquad TR_{g,B} = \frac{1{,}000(\Delta H_{g,B})}{M_w C_{p,g} \Delta T_{ad}}$$

$$St_s = \frac{h a_p L}{(1-\epsilon)\rho_s u_{in} C_{p,s}}; \qquad St_g = \frac{h a_p L}{\epsilon \rho_{g,in} u_{in} C_{p,g}}.$$

The variables that affect the operation of an asymmetric fixed-bed reactor are summarized in the form of appropriate dimensionless groups. The gas Stanton number (St_g) is a measure of the relative magnitude of the rate of convective heat transfer between solids and the gas to the rate of convective heat transfer in the axial direction by the gas. Thus, a higher gas Stanton number indicates a higher axial temperature gradient in the gas phase. The temperature fronts become steeper as the gas Stanton number increases. The solid Stanton number (St_s) is a measure of the relative magnitude of the rate of heat transfer between the gas and the solids compared to the product of the volumetric heat capacity of the solids and the gas velocity. Since the temperature gradient in the solid phase is directly proportional to the rate of heat transfer between the gas and solids, and inversely proportional to the volumetric heat capacity of the solids, a higher solid Stanton number results in steeper temperature fronts in the bed. Because the gas and the solid temperature fronts are known to follow each other closely, a system having higher gas and solid Stanton numbers must involve steeper moving fronts. Thus, the higher the St_s, St_g are, the steeper the temperature fronts in the system.

The dimensionless quantity U is a constant equal to $1/\epsilon$ for incompressible gases, and varies with the gas temperature for compressible gases. The deviation of U from $1/\epsilon$ indicates the variation in the linear velocity of the gas due to its compressible nature. The dimensionless number $\tau_{s/r}$ is the ratio of the space time to the characteristic reaction time. Thus $\tau_{s/r}$ is a Damkohler number for a first-order reaction, and indicates the extent of conversion in the fixed-bed reactor. If $\tau_{s/r} \ll 1$, the conversion in the reactor is negligible and the concentration fronts are flat. If $\tau_{s/r} \gg 1$, nearly complete conversion (or thermodynamic equilibrium for reversible reactions) is achieved in the reactor and the concentration and reaction fronts are very steep.

The dimensionless group TR_g is a measure of the ratio of the enthalpy change caused by reaction in the gas phase to the volumetric gas heat capacity. It indicates the extent of the temperature change in the gas phase due to reaction in the gas phase. If the reaction involved has a very high heat of reaction, the temperature change in the gas phase is very high. A system having high Stanton numbers (St_g and St_s), and high TR_g involves steep temperature fronts, and a system having high $\tau_s/_r$ also involves steep concentration and reaction fronts.

Wrong-way behavior of packed beds

Equations 1–5 were solved first using the algorithm developed by Kulkarni and Duduković (1996a), considering only the exothermic gas-phase reaction ($A \rightarrow C$). Figure 1 illustrates the maximum temperature rise as a function of the inlet gas temperature, and shows that the minimum value of the maximum temperature rise is equal to the adiabatic temperature rise based on the inlet gas temperature and the exit gas conversion. If the initial bed temperature is below or equal to the inlet gas temperature, which is the case if a hot combustible mixture is passed through an initially cold bed, the maximum transient temperature rise ($\Delta T_{g,mx}$) in the bed is equal to the adiabatic temperature rise. However, if the initial bed temperature is moderately higher than the inlet gas temperature, and is sufficiently high to ignite the combustion mixture, the maximum transient temperature rise in the bed is much higher than the adiabatic temperature rise. This phenomenon is known as the *wrong-way behavior* of fixed-bed reactors, and has been reported and studied for catalytic fixed-bed reactors with solid-phase reactions by Kulkarni and Dudukovic (1996b); Il'in and Luss (1992); Chen and Luss (1989): Matros (1989); Pinjala et al. (1988); Mehta et al. (1981); Sharma and Hughes (1976); Van Doesburg and DeJong (1976a,b); and Crider and Foss (1966). We demonstrated it here for gas-phase reactions.

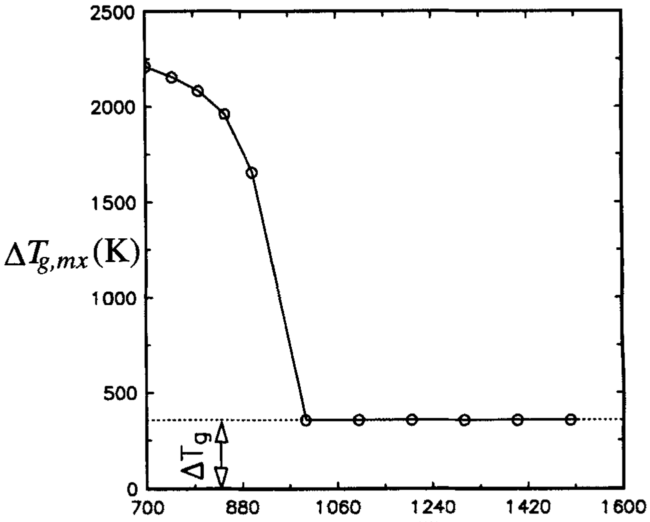

Figure 1. Effect of $T_{g,in}$ on $\Delta T_{g,mx}$ for the gas phase reaction.

As illustrated in Figure 1, the maximum temperature rise in a packed-bed reactor is a dynamic property only for the inlet gas temperatures below the initial bed temperature. Figure 1 indicates that the operating range for a fixed-bed reactor consists of two regimes: a *thermodynamic regime* in which the maximum temperature rise is equal to the adiabatic temperature rise (occurs at gas inlet temperatures equal to or larger than the initial bed temperature), and a *dynamic regime* where the maximum temperature rise depends on the inlet gas temperature (for feed gas temperatures lower than the initial bed temperature). In the *dynamic regime* a low feed temperature decreases the conversion reachable in the upstream section of the reactor where the reactants are getting heated; consequently, the still hot solids in the downstream section are exposed to a higher reactant concentration, leading to an increase in heat generation by reaction, which increases the transient temperature rise in the bed (Il'in and Luss, 1992). This, of course, can happen only when there is interphase heat transfer—in this case, the gas coming into the bed encounters solids that are already hot. In the *thermodynamic regime* the incoming gas is already hotter than the inlet solid temperature, and hence the maximum temperature rise cannot exceed the adiabatic temperature rise. Clearly, the adiabatic temperature rise is always based on the inlet gas temperature.

The rates of endothermic reactions are dramatically enhanced by higher temperatures. Therefore, it seems plausible that the wrong-way behavior of the bed can be utilized to establish high-temperature zones in the bed during a cyclic process, so that the endothermic reaction can undergo completion in a short period of time in such a hot zone. Since a hot zone can be very short, the length of the bed can also be reduced without sacrificing the performance. The goal is to create zones in the bed with temperatures far in excess of the adiabatic temperature of the fuel–air mixture used in the exothermic part of the operating cycle. We now explore conditions under which this can be accomplished.

Sensitivity to the inlet temperature

Based on the results of numerical simulation it was observed that the wrong-way behavior of a fixed-bed reactor is indeed a property that can be exploited in a RE-GAS-type process. Equations 1–5 were solved using implicit finite differences as suggested by Kulkarni and Duduković (1996a), first for a RE-GAS-type process with only gas-phase reactions when solids serve to accumulate and release heat. The exothermic reaction $A \rightarrow C$ takes place during an odd semicycle, and the endothermic reaction $B \rightarrow D$ (with heat of reaction different from that of the exothermic reaction) takes place during an even semicycle. The direction of the feed gases is reversed for each semicycle.

Two different cases of a bidirectional process were studied —one with inlet gas temperature of 700 K and the other with inlet gas temperature of 1,000 K. For both cases the initial bed temperature was 1,000 K. The first period in which only exothermic reaction takes place lasted for 15,000 s, and each subsequent semicycle lasted for 1,000 s. Figure 2 shows the temperature profiles at the end of the first semicycle for both cases. The situation in which the feed temperature is lower than the initial bed temperature is referred to in this article as the *wrong-way process.* The case in which the feed temperature is equal to (or higher than) the initial bed temperature is referred to in the article as the *normal process.* As can be observed from Figure 2, the maximum transient temperature rise for the wrong-way process is more than two times greater than the maximum temperature rise for the normal process, therefore, more than two times greater than the adiabatic temperature rise. Figure 3a shows the temperature profiles in the fixed-bed reactor at the end of the first and of the second semicycle for the wrong-way process. Figure 3b displays the temperature profiles in the fixed-bed reactor at the end of the first and second semicycle for the normal process. As can be observed from Figure 3a and 3b, the maximum temperature rise is higher and the temperature fronts are sharper for

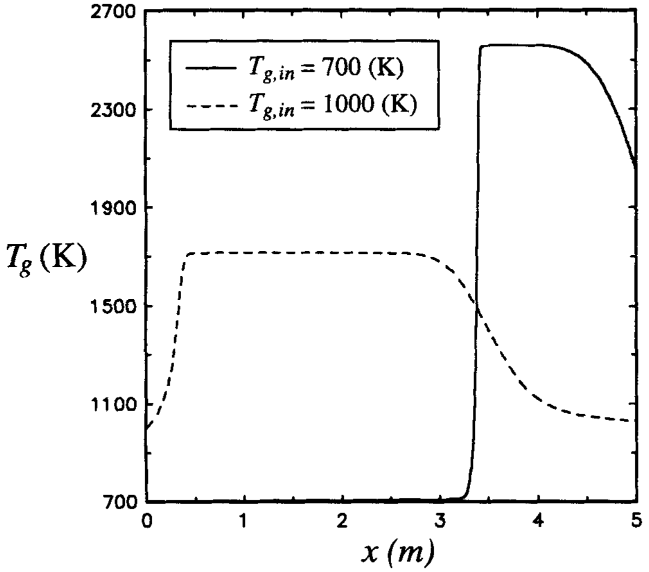

Figure 2. Temperature profile at the end of the first semicycle for the wrong-way and the normal process.

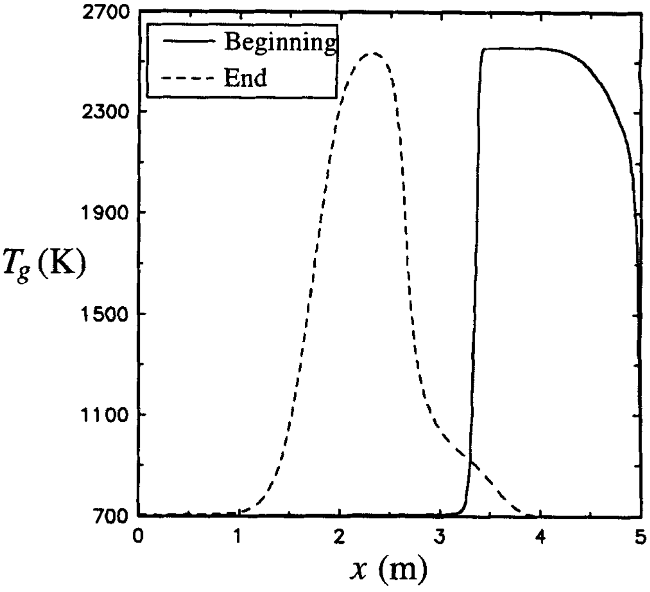

Figure 3a. Gas-phase wrong-way process: temperature profiles at the beginning and end of the second semicycle.

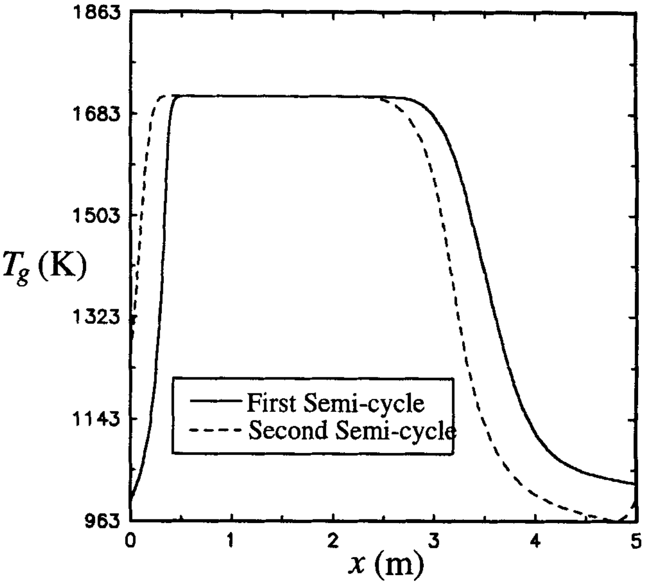

Figure 3b. Gas-phase normal process: temperature profiles at the end of the first and second semicycle.

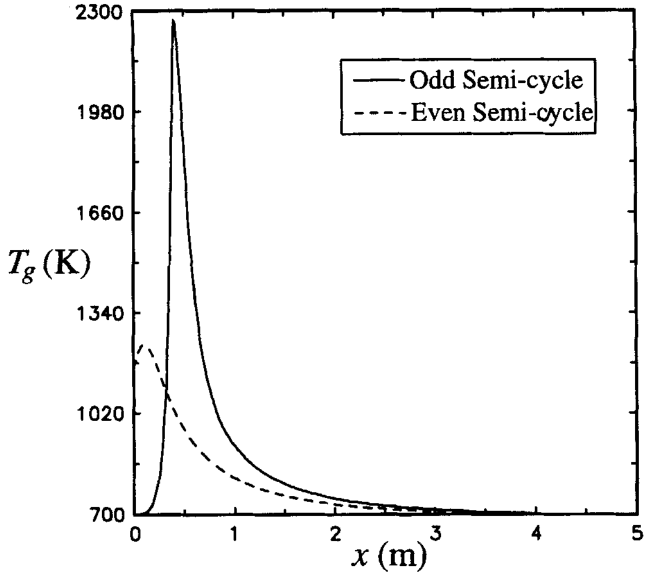

Figure 4a. Gas-phase wrong-way process: the temperature profiles at the pseudo steady state at the end of the semicycle periods.

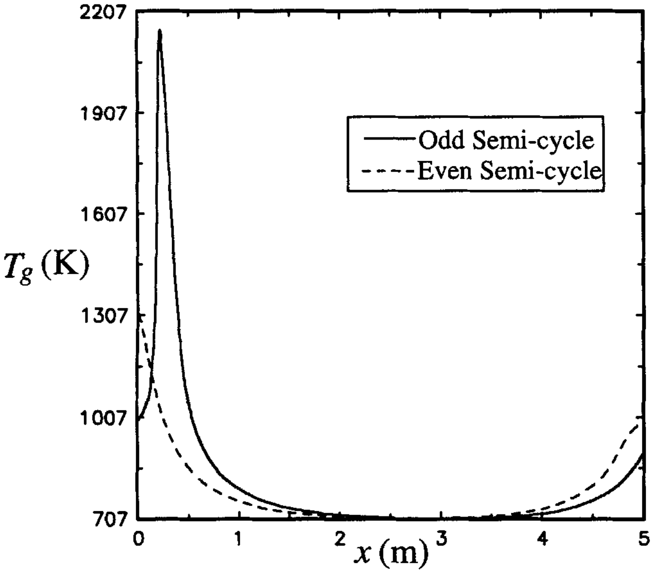

Figure 4b. Gas-phase normal process: the temperature profiles at the pseudo steady state at the end of the semicycle periods.

the wrong-way process. Observe the difference in temperature scale of the ordinate of the two figures. More importantly, during the first semicycle of the wrong-way process, the temperature front moves along the length of the bed with a finite front velocity, and by the end of the first semicycle, which lasted for a period of 15,000 s, the front is well inside the bed (Figure 3a). This gives room for the movement of the front in the opposite direction during the second semicycle. However, in the case of the normal process, the bed gets heated while the temperature front stays stagnant at the entrance (Figure 3b). Since the temperature front stays at the feed end for the first semicycle, right from the beginning of the second semicycle, when the flow is reversed, the temperature front starts moving out of the bed at the feed end of the first semicycle. This implies that even for short even semicycle periods the hot spot can quickly move out of the bed.

Figure 4 and 4b exhibit the pseudo-steady-state temperature profiles at the end of the odd and even semicycles for the wrong-way process and for the normal process, respectively. From Figure 4a and 4b it is evident that the pseudo-steady-state temperature profiles for both the wrong-way process and the normal process are very similar. It can also be observed that the normal process produced the maximum temperature rise in excess of the adiabatic temperature rise (Figure 4b). This occurs because in multiple cycling while advancing toward the pseudo steady state during endothermic (even) semicycles the high-temperature region gets pushed toward the entrance of the bed for the odd (exothermic) semicycles. Hence, at the start of the subsequent odd (exothermic) semicycles the bed temperature in the vicinity of the entrance is higher than the feed temperature, which now allows wrong-way behavior even for the normal process. As can be observed from Figure 4a, the pseudo-steady-state temperature front moved toward the feed end of the odd semicycle ($x = 0$) even for the wrong-way process. Due to the temperature hot spot in the proximity of the feed end for the odd semicycle, during the even semicycles, the hot spot quickly moves out of the bed. This degrades the performance of the wrong-way process and makes it similar to that of the normal process in as much that the exit conversion for the endothermic reaction (even semicycles) is now well below unity as illustrated in Figure 5. Thus, the apparent advantage of the wrong-way process over the normal process during the initial transient operation was lost at the pseudo steady state. This finite creep of the temperature front from first semicycle to pseudo steady state should be avoided to achieve higher

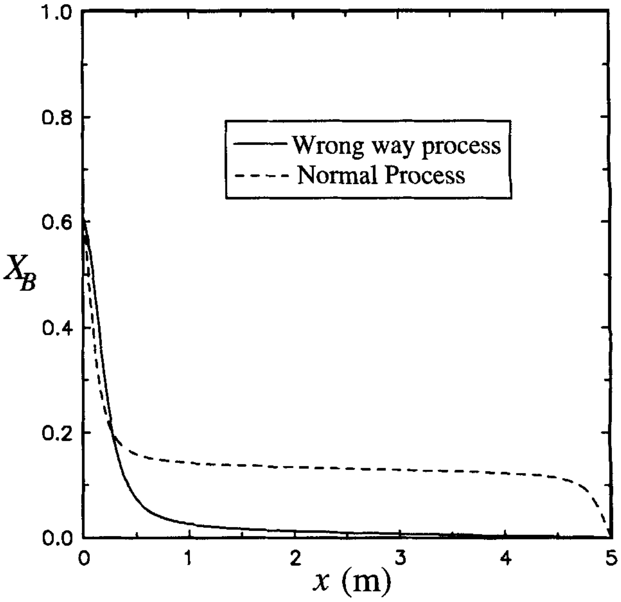

Figure 5. Pseudo-steady-state conversion profiles at the end of two successive even semicycles for the gas-phase wrong-way and normal processes.

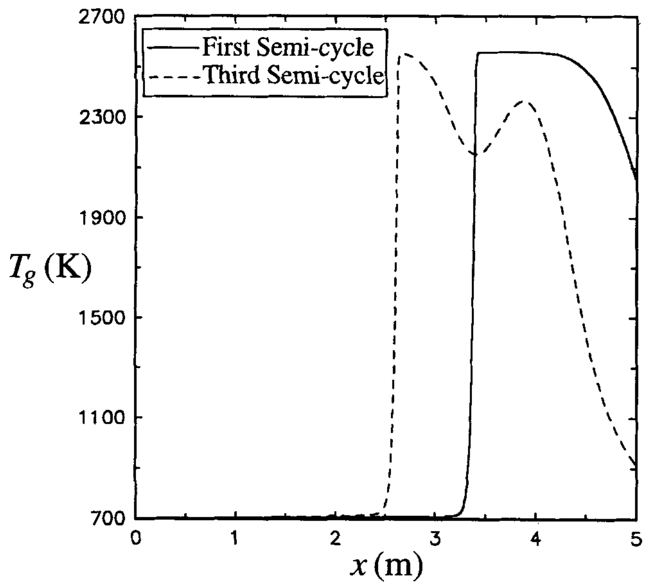

Figure 6. Temperature profiles at the end of two successive early odd semicycles for the wrong-way process.

conversion of the key reactant during the endothermic reaction conducted during the even semicycles. We will now consider how this could be done.

Effect of semicycle periods on the steady state

Differential Creep Velocity. At pseudo steady state, the temperature and the concentration profiles at the beginning or the end of two successive even or odd semicycles should be identical. However, as can be observed in Figure 6, the temperature profiles in repeated cycles prior to establishment of periodic operation, seem to be moving toward the feed end for odd semicycles ($x = 0$) with a certain finite *differential creep velocity*. For the inverted U-shaped temperature profile to exist in the bed at pseudo steady state, the differential creep velocity should be equal to zero. The existence of the finite differential creep velocity indicates that the inverted U-shaped temperature profile will eventually depart the fixed-bed reactor. In the preceding simulation (Figures 6 and 9) the duration of the first semicycle was 15,000 s, and time periods of subsequent semicycles were 5,000 s. The reason for the existence of the differential creep velocity is the difference in the velocities of the fronts during even and odd semicycles. The approximate expression for the front velocity for a single reaction is derived using the coordinate transformation used by Rhee et al. (1973), and is given by

$$\omega_r = \frac{u\rho_g C_{p,g}}{(1-\epsilon)\rho_s C_{p,s}}\left(1-\frac{\Delta T_{ad}}{\Delta T_{mx}}\right) = \omega\left(1-\frac{\Delta T_{ad}}{\Delta T_{mx}}\right). \qquad (6)$$

During an odd semicycle the exothermic reaction takes place with the adiabatic temperature rise equal to 714 K. During an even semicycle the endothermic reaction takes place with the adiabatic temperature drop of approximately -500 K. This results in the difference in the front velocities for odd and even semicycles, with the front velocity for the exothermic reaction (odd semicycle) being lower than that for the endothermic reaction (even semicycle). Since the semicycle period used to generate Figures 2a–4a was constant and set at 1,000 s, and the semicycle period used to generate Figure 6 was a constant set at 5,000 s for both even and odd semicycles, due to faster moving fronts during the even semicycles (i.e., endothermic reaction), the temperature front creeps toward the original feed end of the reactor as the number of cycles increases.

Thus, this difference in the front velocities for the even and odd semicycles is due to the difference in the thermodynamic parameters, namely, the heats of reaction of two different reactions taking place. A bidirectional process can now exhibit a differential front velocity if the inlet velocity, feed composition, and thermodynamic parameters are different for the odd and even semicycles. If in a reverse process, the reactions change with each semicycle, the difference in the front velocity could be appropriately compensated by the difference in the semicycle periods. The simplest criterion for such balanced operation is

$$\frac{\omega_{r,\text{odd}}}{\omega_{r,\text{even}}} = \frac{t^*_{\text{even}}}{t^*_{\text{odd}}}. \qquad (7)$$

The preceding criterion can readily be arrived at from the approximate expression for the differential creep velocity given by Eq. 8, by requiring zero differential creep velocity:

$$\omega_{r,\text{diff}} = \frac{\omega_{r,\text{odd}} \times t^*_{\text{odd}} - \omega_{r,\text{even}} \times t^*_{\text{even}}}{t^*_{\text{odd}} + t^*_{\text{even}}}. \qquad (8)$$

There is another important conclusion that can be drawn from Eq. 6. If the maximum temperature rise in the bed is equal to the adiabatic temperature rise, the front velocity becomes zero, that is, the cold bed gets heated up while the front stays stagnant. It also means that the temperature profile monotonically increases from the feed end during an odd semicycle. If the front velocity is zero for the exothermic reaction, and finite for the endothermic reaction, the front quickly creeps out of the feed end for the odd semicycles.

Discussion of Simulations. Equations 7 and 8 indicate that if the front velocities for even and odd semicycles are not equal to each other, the temperature front can depart the bed. However, as can be observed from Figure 4a, for $t^*_{\text{odd}} = t^*_{\text{even}} = 1{,}000$ s and $\omega_{r,\text{even}} > \omega_{r,\text{odd}}$, this does not happen for the wrong-way process, as the temperature front moves toward the feed end of the odd semicycle during the even semicycle, but partially remains in the bed without completely departing at pseudo steady state. The same bidirectional process was simulated for different bed lengths, and the results are presented in Figures 7 and 8. It is observed, in each case, that during the even semicycle the temperature front moves toward the feed end of the odd semicycle and partially stays in the bed at pseudo steady state. This phenomenon is similar to that of the normal process where the hot spot of the temperature profile stays near the feed end for the odd semicycles from the beginning to end of an odd semicycle, and hence the temperature front partially departs from the bed during even semicycles, as shown in Figure 4b. This causes the exit conversion of the endothermic reaction at pseudo

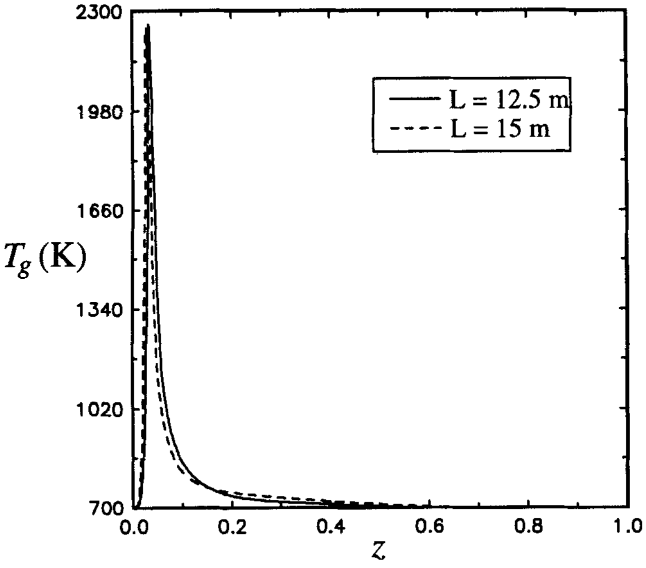

Figure 7. Gas-phase wrong-way process: the pseudo-steady-state temperature profiles at the end of odd semicycles for different reactor lengths.

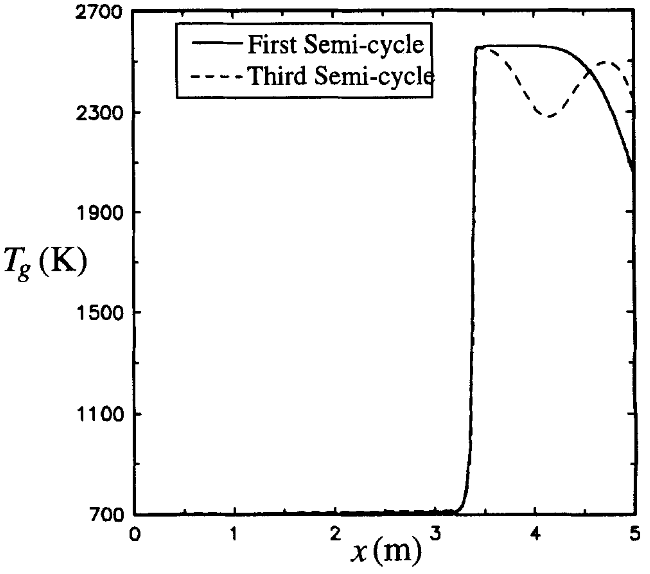

Figure 9. Wrong-way process with adjusted switching periods: the temperature profiles at the end of the first and third semicycles.

steady state, illustrated in Figure 5 both for processes, to be significantly lower than the conversion obtained for the wrong-way process during the initial few cycles. Obviously, at the entrance region of the bed (i.e., $x = 0$), Eq. 6, which is an asymptotic approximation for an infinitely long fixed-bed reactor where no end effects are incorporated (see the Appendix), does not hold. Hence, Eq. 6 is approximate and applicable only to the interior region of the fixed bed reactor where the temperature profile behaves as in an infinitely long bed. Therefore, it is important to have a negligible differential creep velocity in a bidirectional operation. Equation 7 provides an estimate of semicycle periods needed to achieve such negligible differential creep velocity. Since the maximum temperature of the bed also changes between two successive semicycles, the semicycle periods for even and odd semicycles should be determined by trial and error around the values calculated by Eq. 7.

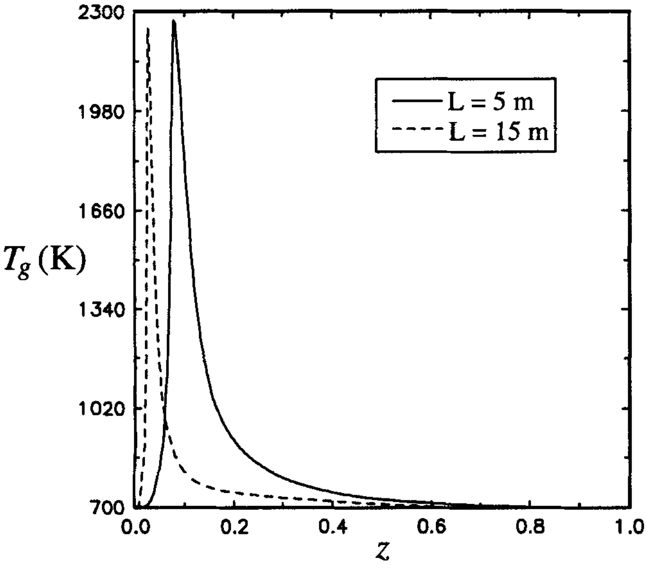

Figure 8. Gas-phase wrong-way process: the pseudo-steady-state temperature profiles at the end of odd semicycles for different reactor lengths.

Based on the kinetic parameters listed in Table 1, the front velocity for the exothermic reaction is calculated. Based on the assumption that an exothermic reaction and an endothermic reaction with the same kinetic and thermodynamic parameters lead to the same front velocity, the front velocity for the endothermic reaction used in the RE-GAS-type process is also calculated. Using these calculations, and some trial and error (see the Appendix), the periods for odd semicycles and for even semicycles were selected to be 1,000 s and 550 s, respectively. The results of the simulation are shown in Figures 9 to 11. As can be seen from these figures, the temperature front now does not display a differential creep velocity and approaches pseudo steady state with an increasing number of cycles. Hence, at dynamic steady state the front traverses from one position in the reactor to the other in a periodic fashion. Also, it can be observed that only the wrong-way process with zero creep velocity results in complete conversion for the endothermic reaction.

Maximum Energy Efficiency. In the processes simulated so far, there is always a finite amount of energy carried out of the bed by the departing gases. This situation always exists if the total heat produced by the exothermic reaction is greater than the total heat absorbed by the endothermic reaction. The energy efficiency of a cycle at pseudo steady state is given by

$$\eta_{\text{cycle}} = \frac{Q_{\text{endo}}}{Q_{\text{exo}}} = \frac{\rho_{gm,in,\text{endo}} u_{in,\text{endo}} X_B \Delta H_{g,B} \times t^*_{\text{even}}}{\rho_{gm,in,\text{exo}} u_{in,\text{exo}} X_A \Delta H_{g,A} \times t^*_{\text{odd}}}. \quad (9)$$

For 100% energy efficiency, the total heat absorbed by the endothermic reaction should be equal to the total heat pro-

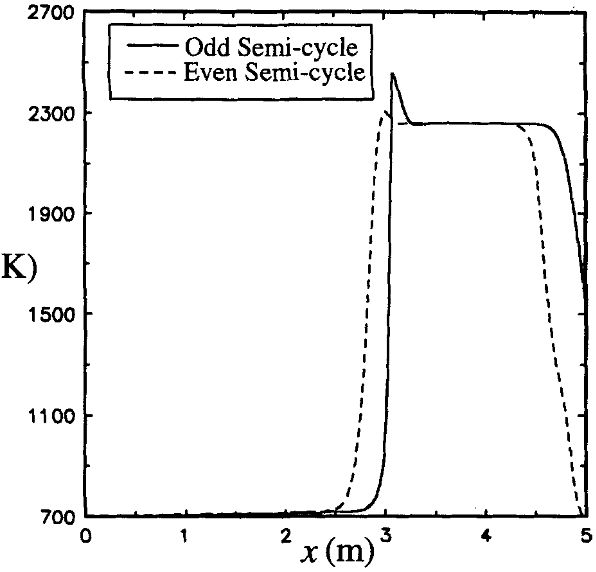

Figure 10. Wrong-way process with adjusted switching periods: the temperature profiles at pseudo steady state.

duced by the exothermic reaction, that is,

$$Q_{\text{exo}} = Q_{\text{endo}}$$
$$\Rightarrow \rho_{gm,in,\text{exo}} u_{in,\text{exo}} X_A \Delta H_{g,A} \times t^*_{\text{odd}}$$
$$= \rho_{gm,in,\text{endo}} u_{in,\text{endo}} X_B \Delta H_{g,B} \times t^*_{\text{even}} \qquad (10)$$

and

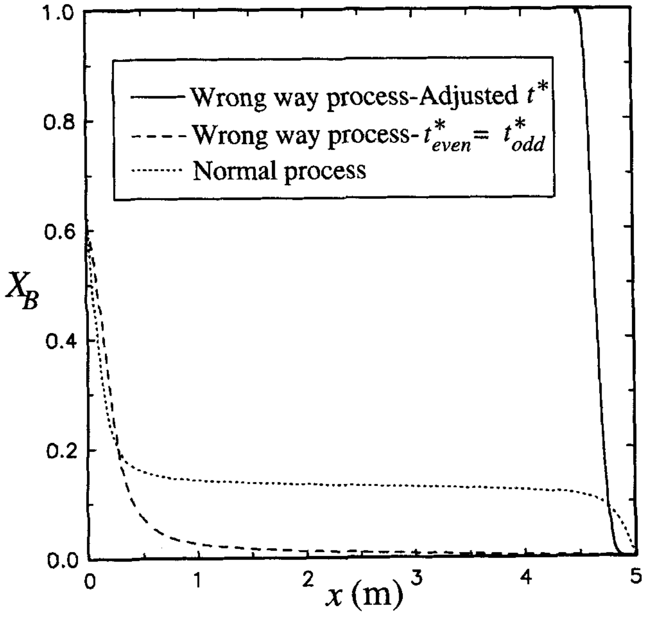

Figure 11. Comparison of conversion profiles at the end of even semicycle for the wrong-way process with adjusted semicycle periods, wrong-way process, and the normal process.

$$\frac{\rho_{gm,in,\text{endo}} u_{in,\text{endo}} X_B \Delta H_{g,B}}{\rho_{gm,in,\text{exo}} u_{in,\text{exo}} X_A \Delta H_{g,A}} = \frac{t^*_{\text{odd}}}{t^*_{\text{even}}}. \qquad (11)$$

Thus, for equal inlet concentrations and temperatures for both exothermic and endothermic reactions, the semicycle periods are determined by the ratio of the heats of reactions.

For the parameters used to simulate the RE-GAS-type process, using Eq. 11, the even and odd semicycle periods were determined to be 1,250 s and 1,000 s, respectively. At pseudo steady state, the temperature profile departed the fixed-bed reactor and no reaction occurred in the bed. This is because the criterion given by Eq. 7 for zero creep velocity is not satisfied by Eq. 11. Obviously, it follows from Eqs. 7 and 11 that 100% energy efficiency can be achieved only when the following relation is satisfied;

$$\frac{\rho_{gm,in,\text{endo}} u_{in,\text{endo}} X_B \Delta H_{g,B}}{\rho_{gm,in,\text{exo}} u_{in,\text{exo}} X_A \Delta H_{g,A}} = \frac{\omega_{r,\text{even}}}{\omega_{r,\text{odd}}} = \frac{t^*_{\text{odd}}}{t^*_{\text{even}}}. \qquad (12)$$

Although Eq. 12 is exact, the expression to estimate front velocity (Eq. 6) is approximate. Hence, front velocities should be determined by trial and error to satisfy Eq. 12. The analysis of the achievable energy efficiency will be discussed elsewhere.

Solid-Phase RE-GAS-Type Process

Model

Here we consider a packed-bed reactor in a RE-GAS-type process with both the exothermic and endothermic reaction occurring in the solid phase. The parametric values used in the computation (Table 1) correspond to a typical combustion–gasification system. The reactions are:

Exothermic: $A \rightarrow C \quad \Delta H_{s,A} < 0 \ldots$ (solid phase)

Endothermic: $B \rightarrow D \quad \Delta H_{s,B} > 0 \ldots$ (solid phase).

Analogously to the gas-phase RE-GAS process, it is assumed that only reaction $A \rightarrow C$ occurs in the bed during an odd semicycle when reactant A is fed to the reactor, and only reaction $B \rightarrow D$ takes place during an even semicycle when B enters from the opposite side of the reactor. The heats of exothermic and endothermic reactions are set to be different (Table 1) to allow for different front speeds during odd and even semicycles.

The same assumptions made in the formulation of the model for the gas-phase RE-GAS-type process are made in the formulation of the model for the solid-phase RE-GAS-type process. The model equations consist of the energy balance for the gas and solid phase, Eqs. 13 and 14, respectively; reactant A, and B mass balances, Eqs. 15 to 16, respectively; and the overall continuity, Eq. 17:

$$\frac{\partial \theta_g}{\partial \tau} = -U \frac{\partial \theta_g}{\partial z} - St_g \frac{1}{\Omega_g} (\theta_g - \theta_s) \qquad (13)$$

$$\frac{\partial \theta_s}{\partial \tau} = \tau_{s/r,s,A} TR_{s,A} \gamma_{s,A}^{((1-\theta_s)/(\theta_g+\theta_{g,d}))} y_A$$
$$+ \tau_{s/r,s,B} TR_{s,B} \gamma_{s,B}^{((1-\theta_s)/(\theta_g+\theta_{g,d}))} y_B + St_s(\theta_g - \theta_s) \qquad (14)$$

$$\frac{\partial y_A}{\partial \tau} = -U\frac{\partial y_A}{\partial z} - \tau_{s/r,s,A}\gamma_{s,A}^{((1-\theta_s)/(\theta_g+\theta_{g,d}))}y_A \tag{15}$$

$$\frac{\partial y_B}{\partial \tau} = -U\frac{\partial y_B}{\partial z} - \tau_{s/r,s,B}\gamma_{s,B}^{((1-\theta_s)/(\theta_g+\theta_{g,d}))}y_B \tag{16}$$

$$\frac{\partial \Omega_g}{\partial \tau} = -\frac{\partial(\Omega_g U)}{\partial z} = 0. \tag{17}$$

The boundary conditions are:

$@\ z = 0$

$\theta_g = \theta_{g,in}; \qquad y_A = y_{A,in}; \qquad y_B = y_{B,in}.$

The initial conditions are:

$@t = 0 \quad \text{and} \quad 0 \le z \le 1$

$\theta_g = \theta_{g,0}; \qquad y_A = y_{A,0}; \qquad y_B = y_{B,0}.$

The dimensionless quantities just used are:

$$\tau = \frac{t}{L/u_{in}}; \qquad z = \frac{x}{L}; \qquad \theta_g = \frac{T_g - T_{g,in}}{\Delta T_{ad}};$$

$$\theta_s = \frac{T_s - T_{g,in}}{\Delta T_{ad}}; \qquad \theta_{g,d} = \frac{2T_{g,in} - T_{g,in}}{\Delta T_{ad}}; \qquad \Omega_g = \frac{\rho_g}{\rho_{g,in}};$$

$$U = \frac{u}{\epsilon u_{in}}; \qquad \gamma_{s,A} = e^{(-Ea_{s,A}/RT_{g,ad})}; \ \gamma_{s,B} = e^{(-Ea_{s,B}/RT_{g,ad})}$$

$$\tau_{s/r,s,A} = \frac{\tau_s}{\tau_{r,s,A}} = \frac{L/u_{in}}{\dfrac{1}{\dfrac{k_{0,s,A}}{(1-\epsilon)}[e^{(-Ea_{s,A}/RT_{g,ad})}]}};$$

$$\tau_{s/r,s,B} = \frac{\tau_s}{\tau_{r,s,B}} = \frac{L/u_{in}}{\dfrac{1}{\dfrac{k_{0,s,B}}{(1-\epsilon)}[e^{(-Ea_{s,B}/RT_{g,ad})}]}}$$

$$TR_{s,A} = \frac{P(-\Delta H_{s,A})}{RT_g\,\rho_s C_{p,s}\Delta T_{ad}}; \qquad TR_{s,B} = \frac{P(-\Delta H_{g,B})}{RT_g\,\rho_s C_{p,s}\Delta T_{ad}}$$

$$St_s = \frac{ha_pL}{(1-\epsilon)\rho_s u_{in}C_{p,s}}; \qquad St_g = \frac{ha_pL}{\epsilon\rho_{g,in}u_{in}C_{p,g}}.$$

The dimensionless group TR_s is a measure of the ratio of the enthalpy change caused by reaction in the solid phase to the volumetric solid heat capacity. It indicates the extent of the temperature change in the solid phase due to the reaction. TR_s is three orders of magnitude smaller than TR_g due to the high volumetric solids heat capacity compared to that of the gas phase. Hence, even if the reaction in the solid phase has a very high heat of reaction, the rate of temperature change in the solid phase due to the heat generated by the reaction is smaller than the rate of change in the temperature of the gas phase if the same reaction were to occur in the gas phase. Because the gas and solid temperatures follow each other quite closely, it is evident that the thermal response of a fixed-bed reactor involving only a solid-phase reaction is much slower than the thermal response of the bed if the same reaction were to occur in the gas phase. The significance of other dimensionless parameters is explained in the section titled "The Gas-Phase RE-GAS-type Process."

Process

The transient response of the bed in which reactions occur in the solids (catalytically) is similar to the case for the gas phase reaction discussed earlier. The phase in which combustion reaction occurs affects the maximum temperature rise. For the same kinetic parameters, the maximum temperature rise in the bed is lower for the solid-phase combustion compared to that for gas-phase combustion. This difference is attributed to the slower dynamics of the solid phase caused by the higher thermal capacity of the solids compared to faster dynamics of the gas phase caused by the lower thermal capacity of the gas. The difference between the maximum temperature rise in the bed for gas-phase combustion and for solid-phase combustion can be very high. Since the rate of increase of the temperature in the bed is slower for a solid-phase reaction, the rate of reaction in the fixed-bed reactor with solid-phase reaction increases slowly before the reactants are depleted. However, in the case of a gas-phase reaction, the rate of change of reaction is sudden, leading to faster production of reaction heat, which increases the transient temperature rise. Due to the fact that the rate of change in the solid phase is slower, in the *dynamic regime*, the maximum temperature rise for the solid-phase reaction is much smaller than that for the gas-phase reaction for the same kinetic parameters. This is shown in Figure 12.

Discussion of simulations

A RE-GAS-type process is simulated here for considering only solid-phase reactions. The parameters used are the same as those used in the simulation of the gas-phase wrong-way process. The temperature profiles for the solid-phase wrong-

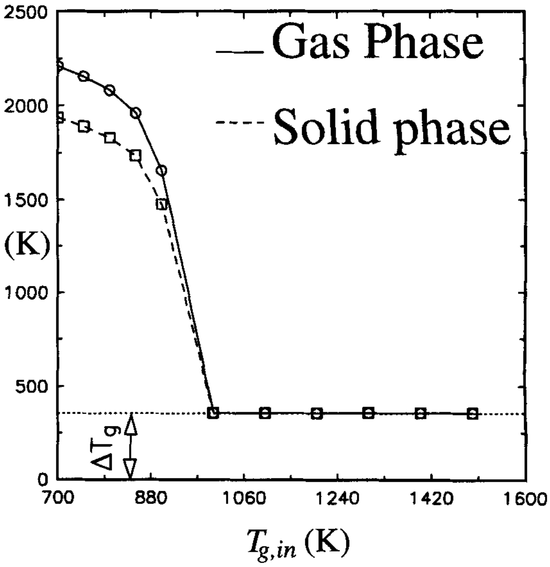

Figure 12. Comparison between wrong-way behavior of fixed-bed reactors with gas-phase and solid-phase reactions.

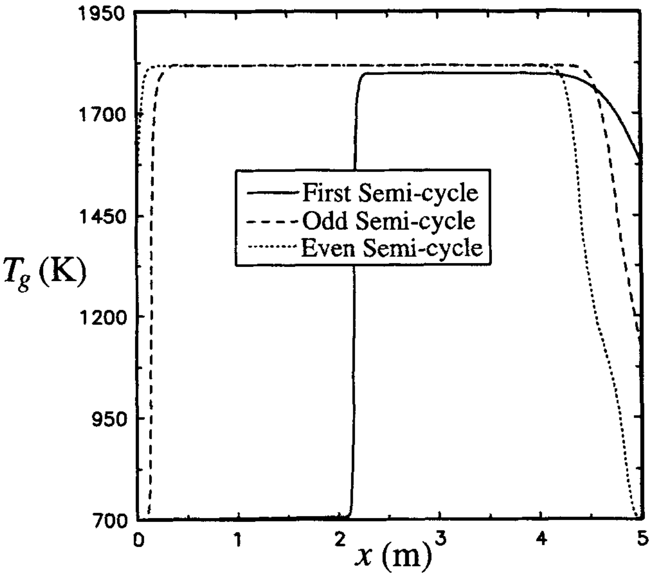

Figure 13. Solid-phase wrong-way process: the temperature profiles at the end of first semicycle and at the end of an odd and even semicycle at the pseudo steady state.

way process are qualitatively similar to those in the case of the gas-phase wrong-way process. Hence, the details of this process are not discussed here. Figure 13 illustrates the temperature profile at the end of the first semicycle and at pseudo steady state. The difference in the thermal response of the bed for the gas-phase and solid-phase reactions is shown in Figure 14. In this figure it is clearly established that the temperature fronts for the gas-phase reaction are much steeper, and that the maximum temperature reached in the fixed bed for gas-phase reactions is much higher.

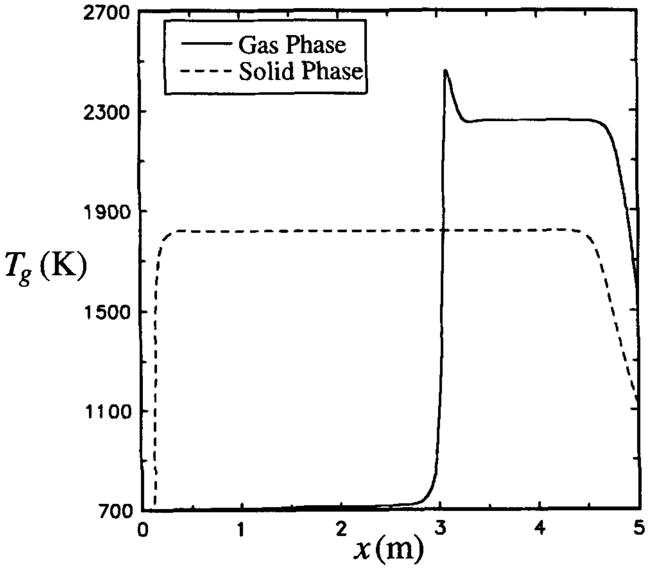

Figure 14. Wrong-way process: the temperature profiles for the gas- and the solid-phase reactions at the end of an odd semicycle at pseudo steady state.

Table 2. Conversion and Thermal Efficiency of Various Processes

Type of Process	X_{endo}	X_{exo}	η_{cycle}
Normal process	0.691	0.882	58%
Wrong-way process	0.807	0.887	68%
Wrong-way process—zero $\omega_{r,diff}$	1.0	1.0	41.3%
Wrong-way process—solid phase (zero $\omega_{r,diff}$)	1.0	1.0	41.3%

A Comparison of the Discussed Processes

The average conversions and energy efficiencies during even and odd semicycles in the various processes discussed in this article are listed in Table 2. It is obvious that the wrong-way process with adjusted semicycle periods to meet the requirement of Eq. 7 for zero creep velocity leads to the highest conversion. The semicycle periods of this process were determined by Eqs. 6 and 7, which require greater t^*_{odd} than t^*_{even} to achieve zero differential creep velocity. This results from Eqs. 6 and 7, which require $t^*_{odd} > t^*_{even}$ when $-\Delta H_{g,A} > \Delta H_{g,B}$, which results in $Q_{exo} > Q_{endo}$. In contrast, the requirement for 100% energy efficiency (Eq. 9) demands t^*_{even} greater than t^*_{odd}. Hence, the thermal energy efficiency of the wrong-way process with adjusted semicycle periods is the lowest of all processes discussed in this article. In this situation, the temperature profile with a well-established hot spot stays well inside the bed, which results in 100% conversion. The wrong-way process with equal odd and even semicycle periods and the normal process yield lower conversion because the hot spot quickly departs from the bed during even semicycles. When it is important to reach high conversions the wrong-way process with adjusted semicycle periods is highly desirable.

Conclusions

The maximum temperature rise and conversion are higher for the wrong-way process (where the inlet gas temperature for the exothermic reaction is below the initial bed temperature), than that for the normal process (where the inlet gas temperature is equal to or greater than the initial bed temperature). The temperature fronts during the odd and even semicycles exhibit different front velocities due to different reactions taking place during the two semicycles. This leads to a net displacement of the inverted U-shaped temperature front after two successive even or odd semicycles. The rate of displacement is given by the differential creep velocity (Eq. 8). To establish a periodically moving temperature front at the pseudo steady state, unequal switching periods given by Eq. 7 should be used. Initially, the normal process does not exhibit a finite front velocity during the heating period, whereas during the cooling period a finite front velocity is displayed. Also, the temperature in the bed monotonically increases during the odd semicycles. During the even semicycles this leads to the quick departure of the high-temperature region from the original feed end of the reactor (i.e., feed end for odd semicycles), which leads to lower conversions during even semicycles.

The maximum energy efficiency is achieved only when total heat generated by the exothermic reaction is equal to the total heat absorbed by the endothermic reaction. The REGAS-type process can operate at 100% efficiency only when Eq. 12 is satisfied.

The gas-phase reactions result in steeper profiles compared to the solid-phase reactions. Also, the maximum temperature rise for the gas-phase reactions is higher than that for the solid-phase reactions. The difference is observed in the dynamics regime and is explained by the higher thermal inertia of the solids compared to that of the gases.

Acknowledgment

The authors are indebted for the support from the industrial participants of the Chemical Reaction Engineering Laboratory (CREL) and the Department of Chemical Engineering that made this work possible.

Notation

a_p = surface-area/bed volume, m^2/m^3
C_p = heat capacity, $J/kg \cdot K$
Ea = activation energy for generic or exothermic reaction, J/mol
h = heat-transfer coefficient, $J/m^2 \cdot K \cdot s$
k = reaction constant, s^{-1}
k_0 = frequency factor, s^{-1}
L = total bed length, m
M_w = molecular weight of the gas
P = total pressure, N/m^2
p = partial pressure, N/m^2
R = universal gas constant, $J/mol. \cdot K$
r = rate of production of, mol/m^3 of bed·s
u = local gas velocity, m/s
X = conversion
x = axial position in the bed, m
y = mole fraction of the gas phase

Greek letters

ΔH = enthalpy of reaction, J/mol
Δt = time step, s
Δy = change in variable y
ϵ = void fraction
τ_s = space time, L/u_{in}
ω = front velocity in a heat regenerator
ρ = density, kg/m^3

Subscripts and superscripts

A = species A
ad = adiabatic
B = species B
cycle = cycle
eq = equilibrium
m = molar
min = minimum
t = time
0 = initial conditions

Literature Cited

Agar, D. W., and W. Ruppel, "Extended Reactor Concept for Dynamic DeNO$_x$ Design," *Chem. Eng. Sci.*, **43**, 2073 (1988).

Blanks, R. F., T. S. Wittrig, and D. A. Peterson, "Bi-Directional Adiabatic Synthesis Gas Generator," *Chem. Eng. Sci.*, **45**, 2407 (1990).

Bunimovich, G. A., N. V. Vernikovskaya, V. O. Strots, B. S. Balzhinimaev, and Yu. Sh. Matros, "SO$_2$ Oxidation in a Reverse-Flow Reactor: Influence of a Vanadium Catalyst Dynamic Properties," *Chem. Eng. Sci.*, **50**, 565 (1995).

Chen, Y. C., and D. Luss, "Wrong-Way Behavior of Packed-Bed Reactors: Influence of Interphase Transport," *AIChE J.*, **35**, 1148 (1989).

Crider, J. E., and A. S. Foss, "Computational Studies of Transients in Packed Bed Tubular Chemical Reactors," *AIChE J.*, **12**, 514 (1966).

Duduković, M. P., and P. A. Ramachandran, "A Moving Finite Element Collocation Method for Transient Problems with Steep Gradients," *Chem. Eng. Sci.*, **39**, 1321 (1984).

Eigenberger, G., and J. B. Butt, "A Modified Crank-Nicolson Technique with Nonequidistant Space Steps," *Chem. Eng. Sci.*, **31**, 681 (1976).

Eigenberger, G., and U. Nieken, "Catalytic Combustion with Periodic Flow Reversal," *Chem. Eng. Sci.*, **43**, 2109 (1988).

Ermenc, E. D., "Wisconsin Process: Pebble Furnace Fixes Atmospheric Nitrogen," *Chem. Eng. Prog.*, **52**(4), 149 (1956a).

Ermenc, E. D., "Wisconsin Process System for Recovery of Dilute Oxides of Nitrogen," *Chem. Eng. Prog.*, **52**(11), 488 (1956b).

Gawdzik, A., and L. Rakowski, "Dynamic Properties of the Adiabatic Tubular Reactor with Switch Flow," *Chem. Eng. Sci.*, **43**, 3023 (1988).

Gawdzik, A., and L. Rakowski, "The Methods of Analysis of Dynamic Properties of the Adiabatic Tubular Reactor with Switch Flow," *Comput. Chem. Eng.*, **13**, 1165 (1989).

Gupta, V. K., and S. K. Bhatia, "Solution of Cyclic Profiles in Catalytic Reactor Operation with Periodic Flow Reversal," *Comput. Chem. Eng.*, **15**, 229 (1991).

Il'in, A., and D. Luss, "Wrong-Way Behavior of Packed-Bed Reactors: Influence of Reactant Adsorption on Support," *AIChE J.*, **38**(10), 1609 (1992).

Jakob, L. M., *Heat Transfer*, Wiley, New York (1957).

Kulkarni, M. S., *Modeling a Heat Regenerator-Reactor with Temperature Dependent Gas Properties*, MS Thesis, Oregon State Univ., Corvallis (1992).

Kulkarni, M. S., and M. P. Duduković, "A Robust Algorithm for Fixed Bed Reactors with Steep Moving Temperature and Reaction Fronts," *Chem. Eng. Sci.*, **51**(4), 571 (1996a).

Kulkarni, M. S., and M. P. Duduković, "Dynamics of Gas Phase and Solid Phase Reactions in Fixed-Bed Reactors," *Chem. Eng. Sci.*, **51**, 3083 (1996b).

Levenspiel, O., "Chemical Engineering's Grand Adventure," *Chem. Eng. Sci.*, **43**, 1427 (1988).

Matros, Yu. Sh., *Catalytic Processes Under Unsteady-State Conditions*, Elsevier, Amsterdam (1989).

Mehta, P. S., W. N. Sams, and D. Luss, "Wrong-Way Behavior of Packed-Bed Reactors: I. The Pseudo-Homogeneous Model," *AIChE J.*, **27**, 234 (1981).

Pinjala, V., Y. C. Chen, and D. Luss, "Wrong-Way Behavior of Packed-Bed Reactors: II. Impact of Thermal Diffusion," *AIChE J.*, **34**, 1663 (1988).

Ramachandran, P. A., and M. P. Duduković, "Solution by Triple Collocation for Periodic Operation of Heat Regenerators," *Comput. Chem. Eng.*, **8**, 377 (1984).

Rhee, H. K., D. Foley, and N. R. Amundson, "Creeping Reaction Zone in a Catalytic Fixed-Bed Reactor: A Cell Model Approach," *Chem. Eng. Sci.*, **28**, 607 (1973).

Sharma, C. S., and R. Hughes, "The Behavior of an Adiabatic Fixed-Bed Reactor for the Oxidation of Carbon Monoxide: II Effect of Perturbations," *Chem. Eng. Sci.*, **34**, 625 (1976).

Schmidt, F. W., and A. J. Willmott, *Thermal Energy Storage and Regeneration*, McGraw-Hill, New York (1981).

Snyder, J. D., and B. Subramaniam, "Numerical Simulation of a Periodic Flow Reversal Reactor for Sulfur Dioxide Oxidation," *Chem. Eng. Sci.*, **48**, 4051 (1993).

Van Doesburg, H., and W. A. DeJong, "Transient Behavior of an Adiabatic Fixed-Bed Methanator: I. Experiments with Binary Feeds of CO and CO$_2$ in Hydrogen," *Chem. Eng. Sci.*, **31**, 45 (1976a).

Van Doesburg, H., and W. A. DeJong, "Transient Behavior of an Adiabatic Fixed-Bed Methanator: II. Methanation of Mixtures of Carbon Monoxide and Carbon Dioxide," *Chem. Eng. Sci.*, **31**, 53 (1976b).

Wallace, K., and H. J. Viljoen, "Modeling of a Monolithic Catalyst with Reciprocating Flow," *AIChE J.*, **41**, 1229 (1995).

Appendix: Analysis of the Temperature and Reaction Front Velocity

The transient temperature and reaction fronts in a fixed-bed reactor spread while moving due to the finite heat-transfer coefficient between the gas and solids and due to mass- and heat-dispersion phenomena. Hence, the assumption of the existence of a constant front velocity is only an approximation. However, assuming such a constant front velocity and the gas to be incompressible, it is possible to analytically find an approximate expression for the approximate rate of the front movement in catalytic packed beds (Rhee et al., 1973). We extend this treatment to homogeneous reactions occurring in a packed-bed regenerator. A single homogeneous first-order reaction is assumed to occur in the gas phase, but the treatment illustrated here remains the same for all types of kinetics. The axial heat dispersion and the radial temperature gradients in the solid phase are neglected. The following model is used for the analysis of the front velocity.

$$\frac{\partial\theta_g}{\partial\tau} = -U\frac{\partial\theta_g}{\partial z} + \tau_{s/r,g,A}TR_{g,A}\gamma_{g,A}^{((1-\theta_g)/(\theta_g+\theta_{g,d}))}y_A - St_g\frac{1}{\Omega_g}(\theta_g-\theta_s) \quad (A1)$$

$$\frac{\partial\theta_s}{\partial\tau} = St_s(\theta_g-\theta_s) \quad (A2)$$

$$\frac{\partial y_A}{\partial\tau} = -U\frac{\partial y_A}{\partial z} - \tau_{s/r,g,A}\gamma_{g,A}^{((1-\theta_g)/(\theta_g+\theta_{g,d}))}y_A. \quad (A3)$$

The boundary conditions are:

$@\ z=0$

$\theta_g = \theta_{g,in};\qquad y_A = y_{A,in}.$

The initial conditions are:

$@\ t=0 \quad \text{and} \quad 0 \le z \le 1$

$\theta_g = \theta_{g,0};\qquad y_A = y_{A,0}.$

The gas heat capacity and the heat-transfer coefficient between the gas and the solids are assumed to be constant and the gas to be incompressible. If the dimensionless front velocity is $V_r = \omega_r/u$ and the length of the fixed-bed reactor is infinite, by using $\xi = z - V_r\tau$, Eqs. A1–A3 can be written as follows:

$$-V_r\frac{\partial\theta_g}{\partial\xi} = -\frac{1}{\epsilon}\frac{\partial\theta_g}{\partial\xi} + \tau_{s/r,g,A}TR_{g,A}\gamma_{g,A}^{((1-\theta_g)/(\theta_g+\theta_{g,d})}y_A - St_g\frac{1}{\Omega_g}(\theta_g-\theta_s) \quad (A4)$$

$$-V_r\frac{\partial\theta_s}{\partial\xi} = St_s(\theta_g-\theta_s) \quad (A5)$$

$$-V_r\frac{\partial y_A}{\partial\xi} = -\frac{1}{\epsilon}\frac{\partial y_A}{\partial\xi} - \tau_{s/r,g,A}\gamma_{g,A}^{((1-\theta_g)/(\theta_g+\theta_{g,d})}y_A, \quad (A6)$$

with

$@\ z=-\infty$

$\theta_g = \theta_{g,in};\qquad \theta_s = \theta_{g,in};\qquad y_A = y_{A,in}$

$@\ z=\infty$

$\theta_g = \theta_{g,mx};\qquad \theta_s = \theta_{g,mx};\qquad y_A = y_{A,eq}.$

Eliminating source terms $\tau_{s/r,g,A}TR_{g,A}\gamma_{g,A}^{((1-\theta_g)/(\theta_g+\theta_{g,d}))}y_A$, $\tau_{s/r,g,A}\gamma_{g,A}^{((1-\theta_g)/(\theta_g+\theta_{g,d}))}y_A$, and $[St_g(\theta_g-\theta_s)]/\Omega_g$ from Eqs. A4–A6 we get

$$V_r\left(St_s\frac{d\theta_g}{d\xi} + St_g\frac{d\theta_s}{d\xi} + St_sTR_{g,A}\frac{dy_A}{d\xi}\right) = \frac{St_s}{\epsilon}\frac{d\theta_g}{d\xi} + \frac{St_sTR_{g,A}}{\epsilon}\frac{dy_A}{d\xi}. \quad (A7)$$

Integrating Eq. A7 from $-\infty$ to ∞ and rearranging, we get

$$V_r = \frac{1}{\epsilon}\frac{1}{1+\dfrac{St_g\Delta\theta_{mx}}{St_s\Delta\theta_{mx}+St_sTR_g\Delta y_{A,mx}}} = \frac{1}{\epsilon}1\Bigg/1+\frac{\dfrac{\Delta T_{mx}}{\epsilon\rho_gC_{p,g}}}{\dfrac{\Delta T_{mx}}{(1-\epsilon)\rho_sC_{p,s}}+\dfrac{1{,}000(-\Delta H_{g,A})\Delta y_{A,mx}}{(1-\epsilon)M_w\rho_sC_{p,s}C_{p,g}}}. \quad (A8)$$

Here the difference between the gas and bed temperatures is ignored. Thus θ and T refer to generic dimensionless and dimensional temperatures, respectively, and Δ indicates the maximum change in the variable.

For a typical system under consideration, an order of magnitude estimate of the variables in Eq. A8 yields

$\Delta T_{mx} \approx 10^2$ or 10^3 K; $\qquad M_w \approx 10^2$ g/mol;

$\rho_g \approx 10^0$ kg/m^3; $\rho_s \approx 10^3$kg/m^3,

$C_{p,g} \approx C_{p,s} \approx 10^3$ J/(kg·K); $\qquad \Delta H \approx 10^5$ or 10^6 J/mol.

Thus,

$$\frac{\Delta T_{mx}}{(1-\epsilon)\rho_sC_{p,s}} + \frac{1{,}000(-\Delta H_{g,A})\Delta y_{A,mx}}{(1-\epsilon)M_w\rho_sC_{p,s}C_{p,g}}$$

is of the order 10^{-3} to 10^{-2} and

$$\frac{\dfrac{\Delta T_{mx}}{\epsilon\rho_gC_{p,g}}}{\dfrac{\Delta T_{mx}}{(1-\epsilon)\rho_sC_{p,s}}+\dfrac{1{,}000(-\Delta H_{g,A})\Delta y_{A,mx}}{(1-\epsilon)M_w\rho_sC_{p,s}C_{p,g}}} \approx 10^2 \gg 1.$$

Therefore Eq. A8 can be rewritten as

$$V_r = \frac{\rho_g C_{p,g}}{(1-\epsilon)\rho_s C_{p,s}} + \frac{1{,}000(-\Delta H_{g,A})(\Delta y_{A,mx})\rho_g}{(1-\epsilon)\Delta T_{mx} M_w \rho_s C_{p,s}}. \quad \text{(A9)}$$

Using the adiabatic energy balance to eliminate the heat of reaction

$$(-\Delta H_{g,A}) = \frac{C_{p,g} M_w \Delta T_{ad}}{1{,}000(-\Delta y_{A,mx})},$$

Eq. A9 can be condensed to the following form:

$$V_r = \frac{\rho_g C_{p,g}}{(1-\epsilon)\rho_s C_{p,s}} \left(1 - \frac{\Delta T_{ad}}{\Delta T_{mx}}\right). \quad \text{(A10)}$$

In dimensional form the front velocity is

$$\omega_r = \frac{u \rho_g C_{p,g}}{(1-\epsilon)\rho_s C_{p,s}} \left(1 - \frac{\Delta T_{ad}}{\Delta T_{mx}}\right) = \omega \left(1 - \frac{\Delta T_{ad}}{\Delta T_{mx}}\right). \quad \text{(A11)}$$

Thus, the temperature front velocity in a fixed bed with reaction is always smaller than the front velocity in the same bed without reaction and is dependent on the ratio of the gas adiabatic temperature rise caused by reaction and the maximum change in the temperature in the bed. A similar expression for the front velocity was obtained by Rhee et al. (1973) for catalytic processes by using a cell model. Thus, the front velocity in a fixed-bed reactor does not change with reaction kinetics or phase in which reaction occurs. It is thermodynamically defined.

Manuscript received Oct. 26, 1995, and revision received Feb. 22, 1996.